Quantifying Simulated Contamination Deposition on Healthcare Providers Using Image Analysis

Lin, Yiqun; Cheng, Adam; Pirie, Jonathan; Davidson, Jennifer; Levy, Arielle; Matava, Clyde; Aubin, Carl-Eric; Robert, Etienne; Buyck, Michael; Hecker, Kent; Gravel, Genevieve; Chang, Todd P

How to cite

LIN, Yiqun et al. Quantifying Simulated Contamination Deposition on Healthcare Providers Using Image Analysis. In: Simulation in healthcare, 2022. doi: 10.1097/SIH.0000000000000664

This publication URL: https://archive-ouverte.unige.ch/unige:161035
Publication DOI: 10.1097/SIH.0000000000000664

Quantifying Simulated Contamination Deposition on Healthcare Providers Using Image Analysis

Yiqun Lin, MD, MHSc, PhD;
Adam Cheng, MD;
Jonathan Pirie, MD, MEd;
Jennifer Davidson, RN;
Arielle Levy, MD, Med;
Clyde Matava, MBChB, MMed, MHSC;
Carl-Eric Aubin, PhD;
Etienne Robert, PhD;
Michael Buyck, MD;
Kent Hecker, PhD;
Genevieve Gravel, MD;
Todd P. Chang, MD, MAcM;
for the INSPIRE Aerosol Generating Medical Procedures (AGMP) Investigators

Introduction: Simulation-based research has played an important role in improving care for communicable diseases. Unfortunately, few studies have attempted to quantify the level of contamination in these simulation activities. We aim to assess the feasibility and provide validity evidence for using integrated density values and area of contamination (AOC) to differentiate various levels of simulated contamination.

Methods: An increasing number of simulated contamination spots using fluorescent marker were applied on a manikin chest to simulate a contaminated healthcare provider. An ultraviolet light was used to illuminate the manikin to highlight the simulated contamination. Images of increasing contamination levels were captured using a camera with different exposure settings. Image processing software was used to measure 2 outcomes: (1) natural logarithm of integrated density; and (2) AOC. Mixed-effects linear regression models were used to assess the effect of contamination levels and exposure settings on both outcome measures. A standardized "proof-of-concept" exercise was set up to calibrate and formalize the process for human subjects.

Results: A total of 140 images were included in the analyses. Dose-response relationships were observed between contamination levels and both outcome measures. For each increment in the number of contaminated simulation spots (ie, simulated contaminated area increased by 38.5 mm^2), on average, log-integrated density increased by 0.009 (95% confidence interval, 0.006–0.012; $P < 0.001$) and measured AOC increased by 37.8 mm^2 (95% confidence interval, 36.7–38.8 mm^2; $P < 0.001$), which is very close to actual value (38.5 mm^2). The "proof-of-concept" demonstration further verified results.

Conclusions: Integrated density and AOC measured by image processing can differentiate various levels of simulated, fluorescent contamination. The AOC measured highly agrees with the actual value. This method should be optimized and used in the future research to detect simulated contamination deposited on healthcare providers.

(*Sim Healthcare* 00:00–00, 2022)

Key Words: Simulation, image analysis, integrated density, area of contamination, fluorescence.

Healthcare simulation has been foundational in the response to communicable disease pandemics, including Ebola,[1–3] H1N1 influenza,[4] and other contaminants.[5,6] One key role of simulation is to optimize the processes of pandemic response for patients, providers, and the healthcare system. For example, studies have used team-based interprofessional in situ simulation to detect latent safety threats and enhance the quality of care.[2,3,5,6] Others have examined strategies to minimize contamination exposure to healthcare workers[7,8] and improve personal protective equipment (PPE) donning and doffing training.[9] Provider exposure to communicable disease poses a serious threat to the viability of the healthcare workforce during a pandemic. Simulation-based research provides a tool to address problems related to this critical issue.

Strategies to quantify measurement of contamination are required to further this type of simulation research. One of the promising methods is to use a particle counter, a precise device that can quantitatively measure the size distribution and number density[10,11] of aerosols particles and droplets in the environment. Particle velocities[12,13] can also be obtained from high-speed visualizations of trajectories. Unfortunately, use of particle counters in simulated clinical environments has substantial

From the KidSIM Simulation Program (Y.L., J.D.), Alberta Children's Hospital; Departments of Pediatrics and Emergency Medicine (A.C.), University of Calgary, Calgary; Pediatric Emergency Medicine Simulation Program (J.P.), The Hospital for Sick Children University of Toronto, Toronto; Departments of Paediatric Emergency Medicine and Paediatrics (A.L., M.B.), University of Montréal Sainte-Justine's Hospital University Centre, Montréal; Department of Anesthesia and Pain Medicine (C.M.), The Hospital for Sick Children, Toronto; Department of Mechanical Engineering (C.-E.A., E.R.), Polytechnique Montréal, Montréal; Department of Veterinary Clinical and Diagnostic Sciences (K.H.), Faculty of Veterinary Medicine University of Calgary, Calgary; Department of Family Medicine and Emergency Medicine (G.G.), Laval University Laval University Hospital Center, Québec City, Canada; and Children's Hospital Los Angeles (T.P.C.), University of Southern California, Los Angeles, CA.

Correspondence to: Yiqun Lin, MD, MHSc, PhD, KidSIM Simulation Research Program, Alberta Children's Hospital, University of Calgary (e-mail: jeffylin@hotmail.com).

A.C. received funding from Canadian Institute of Health Research and INSPIRE research network. Y.L. received funding from Alberta Children's Hospital Research Institute. The other authors declare no conflict of interest.

This study is substudy of a research project financially supported from Canadian Institutes of Health Research (CIHR), International Network for Simulation-based Pediatric Innovation, Research & Education (INSPIRE), and Alberta Children's Hospital Research Institute (ACHRI).

Supplemental digital content is available for this article. Direct URL citations appear in the printed text and are provided in the HTML and PDF versions of this article on the journal's Web site (www.simulationinhealthcare.com).

DOI: 10.1097/SIH.0000000000000664

disadvantages. First, particle counters do not differentiate harmful particles that contain pathogens from normal particles in the environment. Second, particle counters detect droplet and aerosol in the air and not contaminant deposits on surfaces, thus making them a poor option to detect contaminants deposited on healthcare providers. Last, these devices are designed to monitor air quality and therefore only target a size range relevant for suspended particles. Therefore, we require new methods of measurement to quantify the amount of contamination deposition on healthcare providers and surrounding surfaces.

Recently, researchers have used fluorescent markers, such as Glo Germ (Moab, Utah) that illuminate when exposed to UV light to simulate aerosol and droplet contamination.[5,14] The material had been used to improve the efficacy of handwashing[15–17] and demonstrate the ease of person-to-person transfer of contaminants. Therefore, it is ideal to simulate some pathogens that spread through direct contact (eg, Ebola, influenza, and some bacteria). Some recent studies have used fluorescent markers as surrogates of pathogens and studied strategies to mitigate healthcare worker contamination and infection.[5,7–9,14–18] In these studies, photographs are used to document fluorescent splotches or splatter, and the extent of the simulated contamination is only visually assessed by the human eyes.[7,8,14,16–18] Very few studies to date have attempted to quantify the level of simulated contamination.

Image analysis is a promising method to quantify the area and intensity of simulated contamination. Similar technology has been well accepted in the bioimaging informatics,[19] digital immunohistochemistry,[20] and direct immunofluorescence.[21] In this study, we aim to (1) describe 2 simple image analysis methods to quantify simulated contamination created by fluorescent material with available equipment; (2) explore the factors associated with the accuracy of the measurements; and (3) provider proof of concept evidence to demonstrate use of this image analysis method for provider surface contamination.

METHODS

Ethical Considerations

An exemption from ethical review was provided by the Children's Hospital of Los Angeles Institutional Review Board, as no human or animal subjects were involved in this simulation-based study.

Room Settings

We placed a black backdrop at a height of 2 meters and a width of 1.8 meters in a dark room with no windows. The baseline luminance level was less than 0.1 lux as confirmed by a light meter (ANNMETER, ANN-881C, sensitivity 0.1–200,000 lux; Shenzhen, Guangdong Province, China). In front of the backdrop, the torso of a CPR manikin (Resusci Anne QCPR; Laerdal Stavanger, Norway) was placed on top of a table, with the height of the manikin head adjusted to 1.75 meters above the ground, representing the average height of men in Canada.[22] A camera (Powershot G9X Mark II; Canon, Tokyo, Japan) was set approximately 1.3 meters high and 1.3 meters away from the manikin, perpendicular to the backdrop. An UV light (Everbeam, wavelength = 365 nm, power = 50 watts; Zhongshan, Guangdong Province, China) was set beside the camera to illuminate the manikin. The luminance level at the position of the manikin facing the camera was approximately 38 lux, as confirmed by the light meter (Fig. 1).

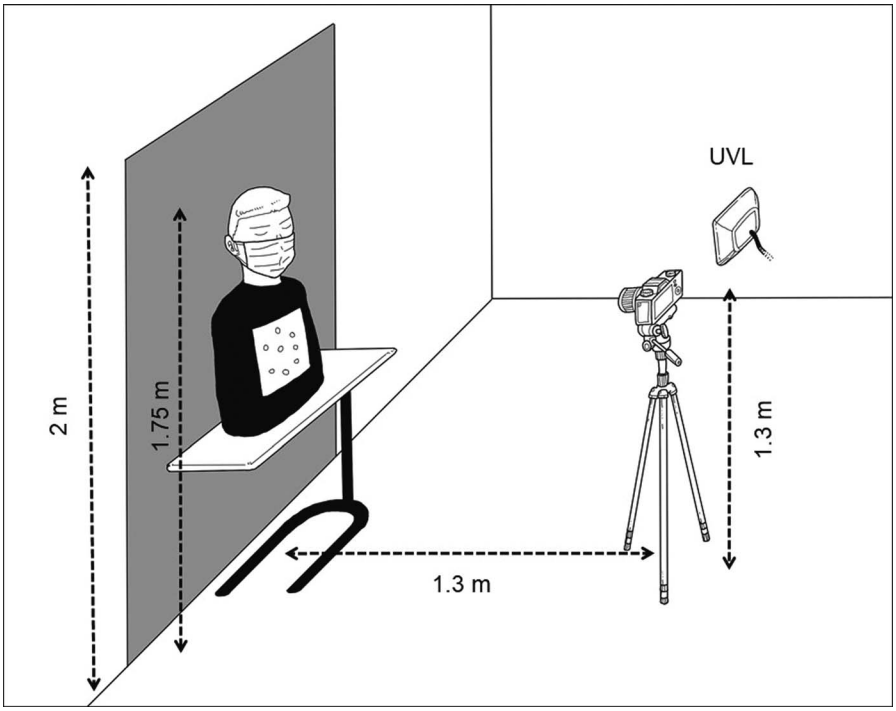

FIGURE 1. Room settings to capture images of simulated contamination. In a dark room with no windows (luminance level <0.1 lux), a black backdrop was placed at a height of 2 meters (high and wide enough to fill the background of the image). A CPR manikin was placed on top of a table, with the height of the manikin head adjusted to 1.75 meters above the ground. A camera was set approximately 1.3 meters high and 1.3 meters away from the manikin, perpendicular to the backdrop. A UV light was set beside and at the same height of the camera to illuminate the manikin. UVL, ultraviolet light.

Simulated Contamination

Simulated contamination spots were created using Glo Germ (Moab) powder, which is a nontoxic fluorescent marker composed of 100% melamine resin visible under UV light. We applied the powder on 150 × 150-mm^2 origami paper to make small identical circular contamination spots (r = 3.5 mm, area = 38.5 mm^2). The detailed procedures to create contamination spots are provided in supplementary digital content 1 (See video, Supplementary Digital Content 1, http://links.lww.com/SIH/A852, procedures to create circular simulated contamination). Five different contamination levels with 0, 1, 3, 7, and 10 contamination spots were set to represent contaminated areas of 0, 38.5, 115.5, 269.4, and 384.8 mm^2, respectively. The actual area of contamination (AOC) was verified using a standardized procedure (See text, Supplementary Digital Content 2, http://links.lww.com/SIH/A853, procedures to verify actual AOC). The contaminated paper was then placed on the chest of the manikin to simulate the contamination deposition on a healthcare worker (Fig. 2).

Camera Exposure Settings

Camera settings would potentially influence image characteristics and ultimately the outcome measures. To address this issue, we standardized several camera setting parameters in this study to avoid confounding factors, such as the distance between the camera and subject (1.3 meters), lens focal length (35 mm) and ISO (400). Lens focal length provides information about how much of the scene will be captured (angle of view) and how large each individual element will be (magnitude), while ISO represents the light gathering ability of a camera (the sensitivity of camera sensor). The aperture controls the amount of light that enters the camera and shutter speed affects the time of the exposure. Both aperture and shutter speed can critically influence the how bright and clear the contaminated spots on the image and outcome measures. We altered aperture and shutter speed in a controlled and standardized fashion to explore how these variables influence our outcome measures. In this study, we used 4 aperture settings (F2.8, F4, F5.6, F8) and 7 shutter speeds (1/30, 1/15, 1/8, 1/4, 1/2, 1, 2 seconds). A total of 140 images were taken (5 different contamination levels × 4 aperture settings × 7 shutter speeds = 140 images) on the same day and saved for image analysis as JPEG format with a dimension of 2432 × 3648 pixels.

Outcome Measures

We used ImageJ, an open-source image processing software designed for multidimensional image processing[23] (https://imagej.nih.gov/ij/), to calculate 2 outcome measures: integrated density value (IDV) and AOC. The IDV is the sum of the gray value in all pixels in the image (ie, product of mean gray value and number of pixels). Gray value is a measure of the brightness of a pixel ranged from 0 to 255 in an 8-bit image (0 as black or completely dark, and 255 as white or very bright). The simulated contamination was fluorescent; therefore, the more area of the contamination, the higher the IDV. Because the distribution of IDV is exponentiated, after natural log transforming the integrated density, the data follow approximately normal distribution to allow parametric statistical analyses.

Area of contamination was calculated using the ImageJ software. After converting the image to greyscale, we selected a region of interest in the image that included all contaminated spots. We then set a scale using length of the origami paper side, so the distance in pixels equivalent to 150 mm was determined. Because the contaminated area was much more brilliant than the noncontaminated area in the image, the pixels representing contaminated areas had relatively higher gray value. After manually adjusting the contrast to enhance the contamination on the image, we were able to define a threshold gray value range that was higher than all the gray values representing noncontaminated area via visual assessment. This method allowed us to separate the contaminated (relatively high gray value pixels) from noncontaminated (relatively low gray value pixels) areas in the image (ie, by highlighting all pixels that have the gray values within that range). The number of pixels highlighted was proportional to AOC with a proportionality constant of the scale we had set. This allowed us to report the AOC as square millimeters. The same investigator (Y.L.) manually adjusted the threshold gray value range depending on the exposure condition of the image and completed all image processing. Detailed procedures of image analysis are provided (see video, Supplementary Digital Content 3, http://links.lww.com/SIH/A854, the demonstration of measuring both integrated density and AOC using ImageJ).

Statistical Analysis

Statistical analyses were conducted using R software[24] (www.r-project.org) with "lme4" packages.[25] Mixed-effects linear regression methods were used to evaluate the effect of contamination level (number of contamination spots) on both natural logarithm of IDV and AOC calculated by ImageJ, adjusting for exposure conditions (ie, aperture and shutter speed). Intraclass correlation coefficient (ICC) and Bland-Altman plots were used to evaluate the agreement between measured and theoretical areas of contamination. An additional linear regression analysis was conducted to explore whether aperture and shutter speed were associated with absolute deviation from theoretical areas of contamination.

Proof-of-Concept Demonstration

To demonstrate the feasibility of implementing the concept and methods in a simulation laboratory, we set up a standardized

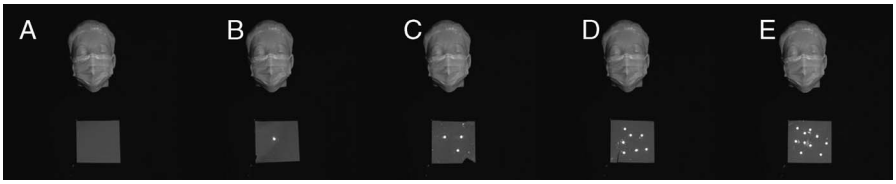

FIGURE 2. Different simulated contamination levels. An example of a set of photos with different simulated contamination levels: (A) no contamination; (B) 1 contamination spot (38.5 mm^2); (C) 3 contamination spots (115.5 mm^2); (D) 7 contamination spots (296.4 mm^2); (E) 10 contamination spots (384.8 mm^2).

contamination exercise using a manikin to calibrate and formalize the process for human subjects. The station was set up in a similar way as described previously. In this demonstration, we used an aperture of 5.6 and a shutter speed of 1/8 seconds. A manikin was dressed in regular PPE and photos were taken in both JPEG format and raw format, with 1 photo as a scale and 4 different settings composed of differing contamination areas and amounts of Glo Germ (Moab) powder used:

(1) Setting 1: No contamination on manikin
(2) Scale: No contamination on manikin, a 20-cm-long ruler applied on the chest
(3) Setting 2: Contamination area of 7 × 7 cm^2 produced with 240-mg powder
(4) Setting 3: Contamination area of 10 × 10 cm^2 produced with 240-mg powder
(5) Setting 4: Contamination area of 10 × 10 cm^2 produced with 480-mg powder

The scale photo was used to calculate AOCs for all the other photos. We present the measured IDV and AOC and compared the results between photos in JPEG format and raw format. Intraclass correlation coefficient was calculated as a measure of agreement between the 2 photo formats. (See figure, Supplemental Digital Content 4, http://links.lww.com/SIH/A855, the settings of "proof-of-concept" demonstration).

RESULTS

Natural Logarithm of IDV—ln(IDV)

As the number of contamination spots increased, the estimated log-IDV [ln(IDV)] increased, and most of the pairwise comparisons to the next larger number of contamination spots demonstrated a statistically significant increase (Table 1). The mixed-effects linear regression model showed that for each increment in the number of contaminated simulation spots, on average, ln(IDV) increased by 0.009 [95% confidence interval (CI), 0.006–0.012; $P < 0.001$; $R^2 = 0.99$]. This association remained statistically significant after adjusting for aperture and shutter speed (see table, Supplementary Digital Content 5, http://links.lww.com/SIH/A856, mixed-effects linear regression model coefficient—factors associated with ln(IDV)). Variance component analysis showed that contamination levels, although statistically significant, only explained 0.1% of the total variance of ln(IDV). Therefore, the outcome of ln(IDV) was very likely to be dramatically influenced by exposure condition, which accounts for 99.5% of the total variance (Table 2).

Area of Contamination by ImageJ

The AOC measured in 4 scenarios (excluding no contamination) was significantly different (Table 3, Fig. 3). The mixed-effects linear regression model showed that for each increment in the number of contaminated simulation spots, on average, the AOC increased by 37.8 mm (95% CI, 36.7–38.8 mm; $P < 0.001$; $R^2 = 0.97$), which is very close to the actual predetermined area (38.5 mm). This association also remained significant after adjusting for aperture and shutter speed (See table, Supplementary Digital Content 6, http://links.lww.com/SIH/A857, mixed-effects linear regression model coefficient—factors associated with AOC). Variance component analysis showed that contamination level explained 99.6% of the total variance of contaminated area, indicating that exposure condition is less likely to influence AOC (Table 2).

The ICC between areas measured by ImageJ and the actual values was 0.978 (95% CI, 0.969–0.985). Bland-Altman plot showed that mean bias between measured and theoretical values was 0.54 mm^2 (1.5%) with a limit of agreement from −55 to 56 mm^2 (−22.2 to 25.2%; See figure, Supplementary Digital Content 7, http://links.lww.com/SIH/A858, Bland-Altman plot of measured and actual AOC). In the linear regression model, factors associated with increased absolute bias were larger contamination area ($P < 0.001$), large aperture ($P = 0.002$), and longer exposure time ($P < 0.001$; see table, Supplementary Digital Content 8, http://links.lww.com/SIH/A859, model coefficients—factors associated with bias of measured AOC).

Proof-of-Concept Demonstration

The integrated density increased with both amount of fluorescent powder used and planned contamination areas (ln(IDV): 17.15, 17.69, 18.05, and 18.08, from setting 1 to setting 4, respectively). The measured AOC changed with the planned contamination area, but not amount of the fluorescent powder used (AOC: 0, 57.1, 112.9, and 108.8, from setting 1 to setting 4, respectively).

The differences in measures between JPEG format and raw format were minimal, with an ICC of 0.99 (see table, supplementary digital content 9, http://links.lww.com/SIH/A860, result and interpretation of proof-of-concept demonstration).

DISCUSSION

In our study, we simulated the process of measuring simulated contamination with a manikin and demonstrated the feasibility of using image analysis to quantify simulated contamination. We have observed a dose-response relationship between level of simulated contamination and both ln(IDV) and

TABLE 1. Mean Differences and Their 95% CIs in Natural Logarithm of IDV in 5 Different Scenarios

MD (95% CI)	Spot = 0	Spot = 1	Spot = 3	Spot = 7	Spot = 10
Spot = 0	0				
Spot = 1	0.027 (−0.004 to 0.059)	0			
Spot = 3	0.035 (0.003 to 0.067) *	0.008 (−0.024 to 0.039)	0		
Spot = 7	0.077 (0.045 to 0.108) *	0.049 (0.018 to 0.081) *	0.042 (0.010 to 0.073) *	0	
Spot = 10	0.096 (0.064 to 0.128) *	0.068 (0.036 to 0.100) *	0.061 (0.029 to 0.093) *	0.019 (−0.013 to 0.051)	0
Estimated ln(IDV)	**17.106 (16.610 to 17.603)**	**17.134 (16.637 to 17.631)**	**17.141 (16.644 to 17.638)**	**17.183 (16.686 to 17.680)**	**17.202 (16.705 to 17.699)**

All values are estimated using mixed-effects linear regression model, number of contamination spot as a categorical variable.
*The mean difference in ln(IDV) from lower number of contamination spots to higher number of spots were statistically significant ($P < 0.05$).
MD, mean difference.

TABLE 2. Variance Component Analysis for 2 Outcome Measures

	Ln(IDV)		Area Measured by ImageJ	
Component	**Variance**	**Percentage**	**Variance**	**Percentage**
Contamination area	0.001	0.1	23,140	96.3
Aperture	0.453	21.3	122	0.5
Shutter speed	1.66	78.2	338	1.4
Residual	0.008	0.4	420	1.8
Total variance explained by contamination		**0.1**		**96.3**
Total variance explained by exposure condition (ie, aperture and shutter speed)		99.5		1.9

AOC measured by ImageJ. Integrated density value was sensitive to changes in exposure settings, while AOC seemed to be minimally affected by camera exposure settings. Area of contamination also achieved excellent agreement between the measured and actual values. Our proof-of-concept demonstration further verified the conclusion. It is worth mentioning that the simple methods proposed in the article are only one of many possible approaches, which is suitable for the simulationist without an engineering background to complete with regular equipment.

The IDV is a measure of total brightness of an image. Although the workload to measure IDV is very low (one click on the software), this outcome measure has a very low "signal-to-noise ratio." Consider the pixels representing contamination as the signal in this case. They have higher gray value (brighter) but constitute a very small proportion only in the image (Fig. 2). The pixels representing the noncontaminated area (noise) are less bright, but the number of pixels is much greater than that of contaminated area. As a result, a subtle change in contaminated area in the image might not yield significant change in the IDV, making it a less sensitive measure to detect small differences in simulated contamination. A stronger exposure condition (ie, large aperture, longer exposure time, and high ISO) could potentially enhance the signal, but unfortunately, it enhanced the noise even further in our study. Therefore, we suggest that researchers use a relatively lower exposure condition to achieve the best signal-to-noise ratio. We recommend that a baseline image is taken before simulation activities when the participant does not have any contamination on their bodies, to quantify the pure noise level of the participant and allow further analysis to filter out the noise. In our study, we found that an aperture of 5.6 and shutter speed of 1/8 seconds achieve the best signal-to-noise ratio (ie, greatest difference in ln(IDV)s between contaminated and noncontaminated settings). However, researchers might need to do pilot work to figure out the optimal settings for their own projects. Because even a slight change in exposure condition could dramatically affect the IDV, it is extremely important to strictly control all the camera exposure (eg, ISO, aperture, shutter speed, focal length) and room settings (eg, standardizing ambient light using an illuminance meter) to avoid measurement bias during assessment.

Compared with IDV, measuring AOC with ImageJ is slightly more complex and requires some basic knowledge of image processing. However, it also comes with advantages. Although IDV and AOC are both clinically important, the interpretation of AOC is more accessible and explicit to most people, because it can be reported in unit of square millimeters. Our results indicated that different exposure conditions of the image did not seem to significantly influence the AOC measure, because the brightness and contrast of each pixel would be manipulated during image process anyway.

Area of contamination does have some disadvantages. First, an accurate scale is required to convert the length in pixels to metric units. This might not always be possible during implementation of simulation research because the scale may not be perfectly straight or not on the same plane as the contamination. This could lead to bias in the outcome measure. In addition, the locations of the camera and the participants should be strictly standardized. In practice, we could ask the participants to apply a scale of a certain length (eg, 20 cm) to their chest at baseline as we have demonstrated. After participating in a simulation scenario (when they have potential contamination deposited on the body), the participants would be asked to stand at the same location where they had their baseline photos taken. The scale obtained at baseline can be used for the subsequent photos. Second, the process of separating the contamination area from the noncontamination area is relatively subjective. Like measurement in ultrasound,[26] people have different approaches to measure a single image, which could be a potential source of error. Therefore, we suggest that researchers provide image processing training to the analysts, who should practice to ensure an appropriate interrater reliability and develop a standard operation procedure to minimize the biases before proceeding to actual research data. Lastly, AOC did not account for intensity of contamination. Different level of contamination of the same area could potentially result in the same AOC in the image analysis.

Although the current image analysis method is a promising way to quantify simulated contamination, it only quantifies the contamination in a 2-dimensional level and works for contamination on a flat surface. While human beings and equipment used during resuscitation have curved surface, that means, some of the contamination might be hidden or overlapped on a single picture. This will inevitably cause measurement

TABLE 3. Area of Contamination Calculated by the ImageJ in 4 Different Scenarios

MD (95% CI)	Spot = 1	Spot = 3	Spot = 7	Spot = 10
Spot = 1	0			
Spot = 3	77.4 (67.3 to 87.5)	0		
Spot = 7	227.2 (217.1 to 237.3)	149.8 (139.7 to 159.9)	0	
Spot = 10	340.5 (330.3 to 350.6)	263.1 (252.9 to 273.3)	113.3 (103.1 to 123.5)	0
Estimated contaminated area, mm	**41.3 (30.8 to 51.7)**	**118.7 (108.2 to 129.1)**	**268.5 (258.0 to 278.9)**	**381.8 (371.3 to 392.2)**

Numbers were estimated using mixed-effects linear regression model, number of contamination spots as a categorical variable.
The mean difference in AOC between the higher number of contamination spots to lower number of spots were statistically significant in all pairwise comparisons.
MD, mean difference.

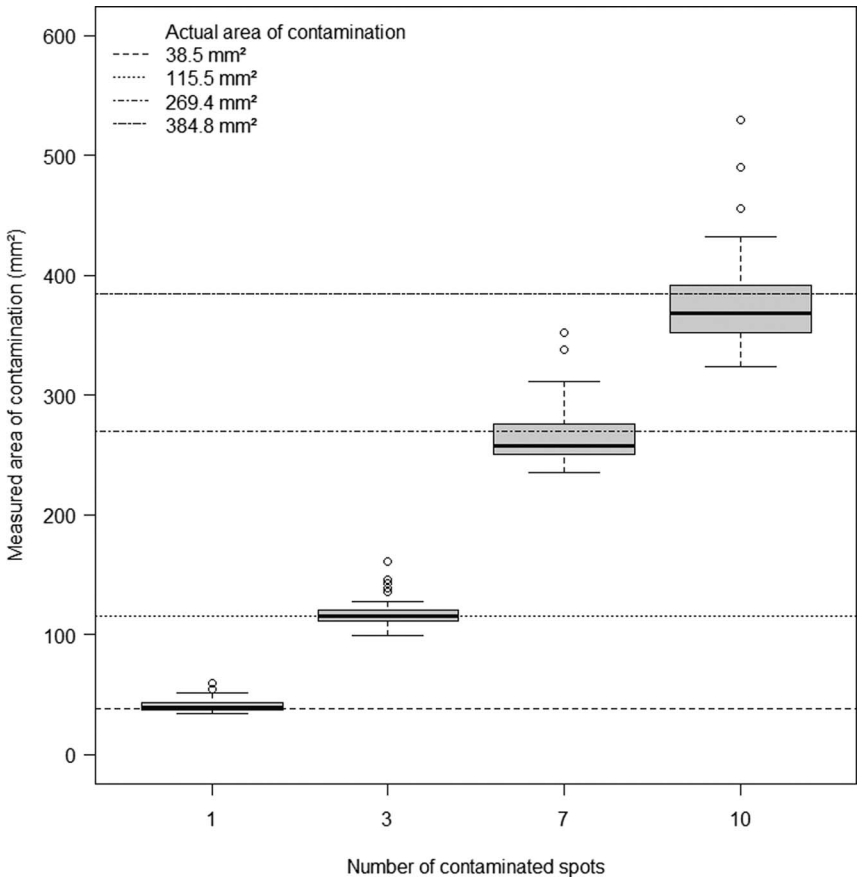

FIGURE 3. Measured AOC in different contamination levels. X-axis, number of contamination spots; Y-axis, measured AOC (in square millimeters); horizontal dot lines represent 4 different actual AOC with 1, 3, 7, and 10 contamination sports; side-by-side boxplots show the distribution of measured AOC (in square millimeters).

errors. Simulation researchers should work with scientists from other fields (eg, computer science, physics, mathematics) to improve and optimize the future process of the measure using technologies like 3-dimensional reconstruction.

Limitations

Our study has several limitations. First, we did not conduct a thorough engineering analysis to determine the spectral sensitivity of our equipment; therefore, the generalizability of the research is limited to the same type of equipment and setup. We acknowledge the methods we proposed in this research were simple. However, we realized that not all simulation researchers will have strong engineering support in their institutions. We hope that the simplicity of the methods will allow all simulation researchers and educators to implement them. Future research should optimize the process and consider techniques like using an optical bandpass filter to improve the signal-to-noise ratios. Second, we manipulated the size of the contaminated areas in this research and did not control for and manipulate the intensity of each contamination spot. The variability of the brightness among different contamination spots was not considered in the linear regression models. Third, we used a CPR manikin with a fixed height and restricted the simulated aerosol contamination to a small area on the chest. In real life, simulation participants are different in sex and body surface, and the AOCs are more dispersed, which might influence the generalizability of the study. Extra work will be required to standardize the location and pose of the participants when implementing this method in the future research. Last, our images were recorded by the camera in JPEG format, which is a compression format resulting in potential loss of digital information in the image and therefore impacting the precision of our results. Although we have demonstrated that the agreement of AOC measurements between the 2 settings was very good, the IDVs were not comparable because of different number of pixels in the pictures. Therefore, we recommend that raw format of photos be used in the future studies.

To implement the proposed methods in the future simulation-based research, investigators need to be aware of a few things. Although the cost of equipment for image analysis protocol proposed was affordable to most institutions (<$800), the time to train the analyst and develop the analysis protocol should not be ignored. Future investigators need to set up a photo taking station similar to our settings and standardize the location of the camera and where the participants stand.

Quantifying levels of contamination using image analysis does open a new path to future simulation research on infectious disease in addition to COVID-19 and can be generalized to other severe infection pathogens that precipitate on surfaces. Despite the limitations, image analysis enables the investigators to objectively measure the performance of the healthcare providers in addition to assessment scores. For example, educators will be able to use simulated contamination areas as a quantitative outcome to measure the amount of contamination

deposited on learners to evaluate different PPE training approaches. This research focuses mainly on the contamination depositions on the healthcare providers; however, it is also possible to measure the contamination deposited on the equipment in a controlled environment (eg, simulation laboratory) with additional standardization protocols. Although extra work is required to make this happen, the information obtained could help hospital administrators improve the education and system process of patient care.

CONCLUSIONS

Both integrated density and AOC measured by ImageJ can differentiate various levels of simulated, fluorescent contamination. Future simulation-based research should consider using these techniques and optimize the process of simulated contamination quantification and ultimately improve the safety of healthcare providers when caring for infectious patients.

ACKNOWLEDGMENT

The authors thank the INSPIRE AGMP Investigators: Mohsen Madadi (Children's Hospital Los Angeles), Guylaine Neveu (University of Montreal), Dana Singer-Harel (The Hospital for Sick Children), Natasha Collia (The Hospital for Sick Children), Jabeen Fayyaz (The Hospital for Sick Children), Brandi Wan (Alberta Children's Hospital), RJ Williams (The Hospital for Sick Children), and Carl Y. Lo (Children's Hospital Los Angeles). The authors also thank Mr Victor Li for his wonderful work of the illustration (Fig. 1) in this article.

REFERENCES

1. Biddell EA, Vandersall BL, Bailes SA, et al. Use of simulation to gauge preparedness for Ebola at a free-standing children's hospital. *Simul Healthc* 2016;11(2):94–99.
2. Phrampus PE, O'Donnell JM, Farkas D, et al. Rapid development and deployment of Ebola readiness training across an academic health system: the critical role of simulation education, consulting, and systems integration. *Simul Healthc* 2016;11(2):82–88.
3. Rojo E, Oruna C, Sierra D, Garcia G, Del Moral I, Maestre JM. Simulation as a tool to facilitate practice changes in teams taking care of patients under investigation for Ebola virus disease in Spain. *Simul Healthc* 2016;11(2):89–93.
4. Brazzi L, Lissoni A, Panigada M, et al. Simulation-based training of extracorporeal membrane oxygenation during H1N1 influenza pandemic: the Italian experience. *Simul Healthc* 2012;7(1):32–34.
5. Drew JL, Turner J, Mugele J, et al. Beating the spread: developing a simulation analog for contagious body fluids. *Simul Healthc* 2016;11(2):100–105.
6. Montauban P, Balakumar C, Rait J, et al. The important role of in-situ simulation in preparing surgeons for the COVID-19 pandemic. *Surgeon* 2021;19(5):279–286.
7. Lockhart SL, Naidu JJ, Badh CS, Duggan LV. Simulation as a tool for assessing and evolving your current personal protective equipment: lessons learned during the coronavirus disease (COVID-19) pandemic. *Can J Anaesth* 2020;67(7):895–896.
8. Matava CT, Yu J, Denning S. Clear plastic drapes may be effective at limiting aerosolization and droplet spray during extubation: implications for COVID-19. *Can J Anaesth* 2020;67(7):902–904.
9. Osei-Bonsu K, Masroor N, Cooper K, et al. Alternative doffing strategies of personal protective equipment to prevent self-contamination in the health care setting. *Am J Infect Control* 2019;47(5):534–539.
10. Fidler RL, Niedek CR, Teng JJ, et al. Aerosol retention characteristics of barrier devices. *Anesthesiology* 2021;134(1):61–71.
11. Wilson NM, Marks GB, Eckhardt A, et al. The effect of respiratory activity, non-invasive respiratory support and facemasks on aerosol generation and its relevance to COVID-19. *Anaesthesia* 2021;76(11):1465–1474.
12. Patel SH, Yim W, Garg AK, Shah SH, Jokerst JV, Chao DL. Assessing the physiological relevance of cough simulators for respiratory droplet dispersion. *J Clin Med* 2020;9(9):3002.
13. Simpson JP, Wong DN, Verco L, Carter R, Dzidowski M, Chan PY. Measurement of airborne particle exposure during simulated tracheal intubation using various proposed aerosol containment devices during the COVID-19 pandemic. *Anaesthesia* 2020;75(12):1587–1595.
14. Moulthrop AJ, Kolarczyk LM, Teeter EG. Preventing contamination during transesophageal echocardiography in the face of the coronavirus disease 2019 (COVID-19) pandemic: a Glo Germ experience. *J Cardiothorac Vasc Anesth* 2021;35:2824–2826.
15. Konicki T, Miller E. Use of a simulation intervention to examine differences in nursing students' hand hygiene knowledge, beliefs, and behaviors. *Nurse Educ Today* 2016;45:96–101.
16. Kisacik OG, Cigerci Y, Gunes U. Impact of the fluorescent concretization intervention on effectiveness of hand hygiene in nursing students: a randomized controlled study. *Nurse Educ Today* 2021;97:104719–104719.
17. Öncü E, Vayısoğlu SK. Duration or technique to improve the effectiveness of children' hand hygiene: a randomized controlled trial. *Am J Infect Control* 2021;49:1395–1401.
18. Noor Azhar M, Bustam A, Poh K, et al. COVID-19 aerosol box as protection from droplet and aerosol contaminations in healthcare workers performing airway intubation: a randomised cross-over simulation study. *Emerg Med J* 2021;38(2):111–117.
19. Eliceiri KW, Berthold MR, Goldberg IG, et al. Biological imaging software tools. *Nat Methods* 2012;9(7):697–710.
20. Laurinaviciene A, Plancoulaine B, Baltrusaityte I, et al. Digital immunohistochemistry platform for the staining variation monitoring based on integration of image and statistical analyses with laboratory information system. *Diagn Pathol* 2014;9(suppl 1):S10.
21. Chessel A. An overview of data science uses in bioimage informatics. *Methods* 2017;115:110–118.
22. Wikipedia. Average human height by country. Available at: https://en.wikipedia.org/wiki/Average_human_height_by_country. Accessed May 9, 2021.
23. Schneider CA, Rasband WS, Eliceiri KW. NIH image to ImageJ: 25 years of image analysis. *Nat Methods* 2012;9(7):671–675.
24. *R: A Language and Envionment for Statistical Computing* [computer program]. Vienna, Austria: R Foundation for Statistical Computing; 2017.
25. Bates D, Maechler M, Bolker B, Walker S. Fitting linear mixed-effects models using lme4. *J Stat Softw* 2015;67(1):1–48.
26. Sarris I, Ioannou C, Chamberlain P, et al. Intra- and interobserver variability in fetal ultrasound measurements. *Ultrasound Obstet Gynecol* 2012;39(3):266–273.